SI Materials and Methods

Cell culture and plasmids. 293T, ES-2, OVCAR3, SKOV3, and TOV-21G cell lines were purchased from the American Type Culture Collection (ATCC; Manassas, VA, USA), A2780 cells were derived from the National Experimental Cell Resource Sharing Platform (Beijing, China), and 3AO cells were purchased from the Cell Bank of the Chinese Academy of Sciences (Shanghai, China). The OVCA433 and OVTOKO cell lines were gifts from Professor Zhigang Zhang (Shanghai Jiao Tong University), and OVCA432 cells were kindly provided by Professor Zhe Liu (Tianjin Medical University). 293T cells were cultured in DMEM supplemented with 10% foetal bovine serum (FBS), OVCAR3 cells were cultured in RPMI1640 supplemented with 20% FBS, SKOV3 cells were cultured in McCoy's 5A supplemented with 10% FBS, and all the other cell lines were maintained in RPMI 1640 supplemented with 10% FBS. All cell lines were authenticated using short tandem repeat (STR) DNA fingerprinting routinely and were tested by MycoBlue Mycoplasma Detector (Vazyme Biotech, Nanjing, China) to exclude Mycoplasma contamination before being used for any experiments. The four ovarian cancer primary cell lines OVP1, OVP2, OVP3 and OVM1 were established via sterile processing of fresh tumour biopsy specimens from patients at the time of primary resection. According to the manufacturer's protocol of the Cell Suspension Isolation Kit from Fresh/Frozen Tissues (Invent, Plymouth, MN, USA), tumours were mechanically disrupted, enzymatically digested and filtered through 100 μm filter to obtain single-cell suspensions (cell line characteristics and tissue sources are

described in Table S2). Primary cells were cultured in DMEM supplemented with 20% FBS and were used within 10 passages.

The 66 retrovirus-based FLAG-HA tagged deubiquitinase plasmids were ordered from Addgene (Cambridge, MA, USA). The USP9X plasmid (H3410) was purchased from FulenGen (Guangzhou, China). Full-length or truncated cDNAs were constructed by PCR amplification with specific primers and restriction sites, subsequently cloned into the pLVX-IRES-neo vector and verified by DNA sequencing. The DUB3^{C89S} mutant was generated using a Q5® Site-Directed Mutagenesis Kit (New England Biolabs, Ipswich, MA, USA) in accordance with the manufacturer's protocol. MCL1^{13R} plasmid (all lysines replaced with arginines) was generated by gene synthesis (Beijing Genomics Institute, China). shRNA targeting sequences were cloned into the pSIH-H1 vector. The DUB3 shRNA sequences were as follows (5'-3'): sh1, GGAGATCCAAAGGGAAGAA and sh2, GTGAGAGTGTGTCAAGAGGCAG. The MGMT shRNA sequences were as follows (5'-3'): sh1, GAGCAGGGTCTGCACGAAATA and sh2, TGAGCGACACACACGTGTAAC. The following non-targeting shRNA sequence was used as a negative control (5'-3'): AGTCTTAATCGCGTATAAGGC. Transient transfection of plasmids was performed using Lipofectamine 2000 reagent (Invitrogen, Carlsbad, CA, USA) according to the manufacturer's instructions.

Antibodies and reagents. Antibodies used for immunoblotting, immunoprecipitation, immunochemistry and immunofluorescence in this study were as follows: DUB3, 1:500 (IB), 1:100 (IHC; HPA045642, Sigma); MCL1, 1:1000 (IB), 1:100 (IP and IHC), 1:200

(IF; Abcam, ab32087); V5, 1:1,000 (IB; ab27671, Abcam); V5, 1:800 (IF; #13202, Cell Signaling), HA, 1:5,000 (IB; ab9110, Abcam), FLAG, 1:1000 (IB; #8146, Cell Signaling Technology), Myc, 1:2000 (IB), 1:200 (IP; M047-3, MBL); rabbit IgG (IP; #2729, Cell Signaling Technology); β-actin 1:3000 (IB; A5316, Sigma); PARP, 1:1000 (IB; #9542, Cell Signaling Technology); Cleaved Caspase-3, 1:1000 (IB; #9664, Cell Signaling Technology), BCL-2 1:1000 (IB; #4223, Cell Signaling Technology); BCL-W 1:1000 (IB; #2724, Cell Signaling Technology); BCL-XL 1:1000 (IB; #2764, Cell Signaling Technology); BAK 1:1000 (IB; #12105, Cell Signaling Technology); BAX 1:1000 (IB; #5023, Cell Signaling Technology); USP9X 1:1000 (IB; #14898, Cell Signaling Technology); USP13 1:1000 (IB; ab109264, Abcam); and MGMT, 1:1000 (IB; ab108630, Abcam). Cycloheximide (C7698) and MG132 (C2211) were purchased from Sigma (St. Louis, MO, USA). All inhibitors used in this study were bought from MCE (NJ, USA) and are listed in detail in Table S3.

Quantitative real-time PCR (qRT-PCR). Total RNA was isolated from cells using TRIzol reagent (Thermo Scientific, Grand Island, NY, USA) and then reverse transcribed to cDNA using a Quantscript RT Kit (Tiangen, Beijing, China). The qRT-PCR analysis was performed on a StepOnePlus Real-Time PCR system (Applied Biosystems (ABI), Foster City, CA, USA) using standard procedures. All relative expression levels of the target genes were normalized to those of GAPDH, which served as an endogenous control. The DUB3 (HQP011104) and MCL1 (HQP010025) primers used in the qRT-PCR analyses were purchased from FulenGen (Guangzhou, China). The GAPDH primers were as follows: forward, 5'-

CCGGGAAACTGTGGCGTGATGG-3'; reverse, 5'-AGGTGGAGGAGTGGGTGTCGCTGTT-3'. The MGMT primers were as follows: forward, 5'-ACCGTTTGCGACTTGGTACTT-3'; reverse, 5'-GGAGCTTTATTTCGTGCAGACC-3'.

Mass spectrometry. Flag-DUB3 transiently overexpressed in 293T cells was immunoprecipitated with anti-Flag M2 affinity gel and eluted with 1×loading buffer. Eluted proteins were identified with a gel-based liquid chromatography-tandem mass spectrometry (Gel-LS-MS/MS) approach (Beijing Qinglian Biotech Co., Ltd., China). Mass spectra were analyzed using Maxquant software (version 1.5.3.30) with the UniProtKB/Swiss-Prot human database.

Immunoprecipitation and Western blotting. Cell samples were lysed with RIPA lysis buffer supplemented with a protease inhibitor cocktail (Roche, Basel, Switzerland) for 20 minutes on ice and were then centrifuged at 14,000 g for 10 minutes. The supernatants were collected, and the total protein concentrations were determined using a BCA kit (Thermo Scientific). For Immunoprecipitation, equal amounts of lysate were incubated with anti-FLAG M2 affinity gels (A2220, Sigma) or anti-V5-tag pAb-agarose (D291-8, MBL, Japan) or with protein A/G magnetic beads (HY-K0202, MCE) and either anti-MCL1 antibody or anti-Myc antibody overnight at 4°C. Thereafter, the beads were washed three times with cell lysis buffer, and the immunoprecipitated proteins were analyzed with Western blotting. The samples were separated on 6%, 10% or 15% gels depending on the molecular weights of the targets, and then the proteins were transferred onto PVDF membranes (Merck Millipore, Billerica, MA, USA).

***In vivo* deubiquitination assay.** The *in vivo* deubiquitination assay was carried out in 293T cells. HA-Ub and FLAG-MCL1 were co-transfected with empty vector, V5-DUB3 or V5-DUB3^{C89S} plasmid as indicated. The cells were treated for 6 h with 20 mM MG132 at 48 h post-transfection and then lysed. Proteins in the cell lysate were immunoprecipitated to isolate ubiquitinated MCL1, which was detected with an anti-HA antibody.

Immunofluorescence staining. Cells were seeded into a μ-Slide V1 (ibidi, Germany) and cultured for 24 h. After being fixed with 4% paraformaldehyde and permeabilized by Triton X-100, the cells were blocked by 3% BSA and then incubated with primary antibodies overnight. Proteins were visualized by incubation with anti-mouse IgG conjugated with Alexa Fluor 488 (#4412, Cell Signaling Technology) or anti-rabbit IgG conjugated with Alexa Fluor 594 (#9854, Cell Signaling Technology) and stained with Hoechst 33342 (Thermo Scientific) for 10 minutes, after which the cells were imaged under a fluorescence microscope.

Flow cytometry. Flow cytometry was performed using an apoptosis detection kit (Dojindo, Tokyo, Japan) as previously described according to the manufacturer's protocol (1).

TUNEL staining. Cell apoptosis was determined using a TUNEL Andy Fluor 488 Apoptosis Detection Kit (GeneCopoeia, MD, USA) as previously described following the manufacturer's protocol (1).

CCK-8 cell proliferation and cell viability assays. CCK-8 reagent (Dojindo) was added to the cell culture medium at a ratio of 1:10, and after the cells were incubated for 1 h at 37°C, the absorbance was measured at 450 nm. For the cell proliferation assay, 2×10^3 ovarian cancer cells were seeded into 96-well microplates, and one plate was measured each day for five consecutive days. The relative cell proliferation rate was calculated by normalizing the absorbance at 450 nm on days 2-5 to the absorbance detected on the first day. For the cell viability assay, 1×10^4 ovarian cancer cells were seeded into 96-well microplates, drugs were added after cell adhesion, and cell viability was detected 24 h later as in the proliferation assay. Cell viability was calculated by normalizing the absorbance at 450 nm of the experimental groups to that of the negative control group.

Animal experiments. All animal protocols were approved by the Animal Care and Use Committee of the Chinese Academy of Medical Sciences Cancer Hospital. For the animal experiments showed in Fig. 3*D* and *E* and Fig. S4*E* and *F*, 3×10^6 fluorescently labeled 3AO cells were peritoneally injected into 6-week-old female BALB/c nude mice (Nanjing Biomedical Research Institute of Nanjing University, Nanjing, China). Six days later, saline, 20 mg kg^{-1} or 40 mg kg^{-1} CBP was administered by intraperitoneal injection every three days. Twelve days later, these mice were anesthetized and treated with fluorescein to enable *in vivo* fluorescent imaging. Eighteen days later, another *in vivo* fluorescent imaging experiment was performed. Thirty days later, these mice were harvested to count the number of celiac tumors. For subcutaneous xenografting, 3×10^6 ovarian cancer cells were subcutaneously implanted into 6-week-

old female BALB/c nude mice. For the animal experiments showed in Fig. 3*F* and Fig. S4*I* and *J*, saline or 30 mg kg^{-1} CBP was peritoneally injected every three days beginning six days after cell xenograft. For the animal experiments showed in Fig. 4*D* and *E* and Fig. S7*E*-*H*, Saline, 40 mg kg^{-1} CBP, or 20 mg kg^{-1} PaTrin-2 was peritoneally injected for 5 consecutive days beginning six days after cell xenograft. The tumor lengths and widths were measured every three days with a caliper, and the tumor volume was calculated with the formula $0.52 \times length \times width^2$. After tumors had grown for the designated time, all the mice were euthanized, and the tumors were harvested.

Statistics. Unless otherwise indicated, all statistical results represent the mean±s.d., and statistical comparisons between groups were performed using the two-tailed Student's *t*-test. For all statistical analyses, differences for which $P \leq 0.05$ were considered statistically significant, and at least three biologically independent experiments with similar results are reported. The data analysis was performed using GraphPad Prism version 6.01 (San Diego, CA, USA).

References

1. Luo Q*, et al.* (2018) ARID1A ablation leads to multiple drug resistance in ovarian cancer via transcriptional activation of MRP2. *Cancer Lett* 427:9-17.

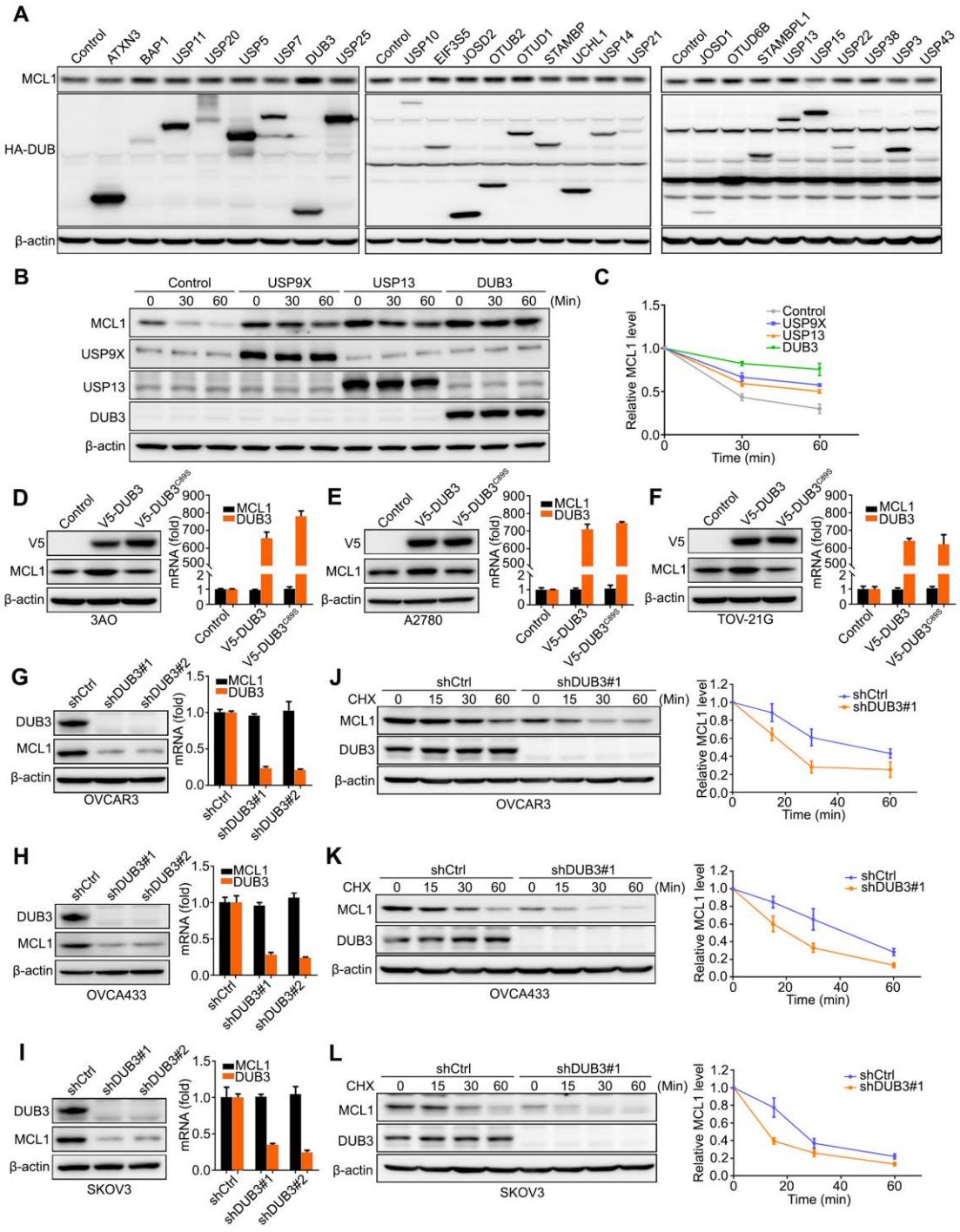

Fig. S1 DUB3 stabilizes MCL1 protein. (*A*) Representative results of immunoblotting of endogenous MCL1 after individually transfecting 66 DUBs into 293T cells. (*B* and *C*) Immunoblotting and quantification of MCL1, USP9X, USP13, and DUB3 expression in a CHX pulse-chase assay. (*D-F*) Immunoblotting and qRT-PCR detection of MCL1 expression in 3AO, TOV-21G and A2780 cells expressing DUB3 or DUB3^{C89S}. (*G-I*) Immunoblotting and qRT-PCR detection of MCL1 expression in OVCAR3, OVCA433 and SKOV3 cells expressing non-targeting shRNA or shRNAs targeting DUB3. (*J-L*) Immunoblotting of MCL1 expression and quantification of MCL1 expression relative to β-actin expression in OVCAR3, OVCA433 and SKOV3 cells expressing non-targeting or DUB3-targeting shRNAs in a CHX pulse-chase assay. The error bars indicate the mean±s.e.m of three biological replicates.

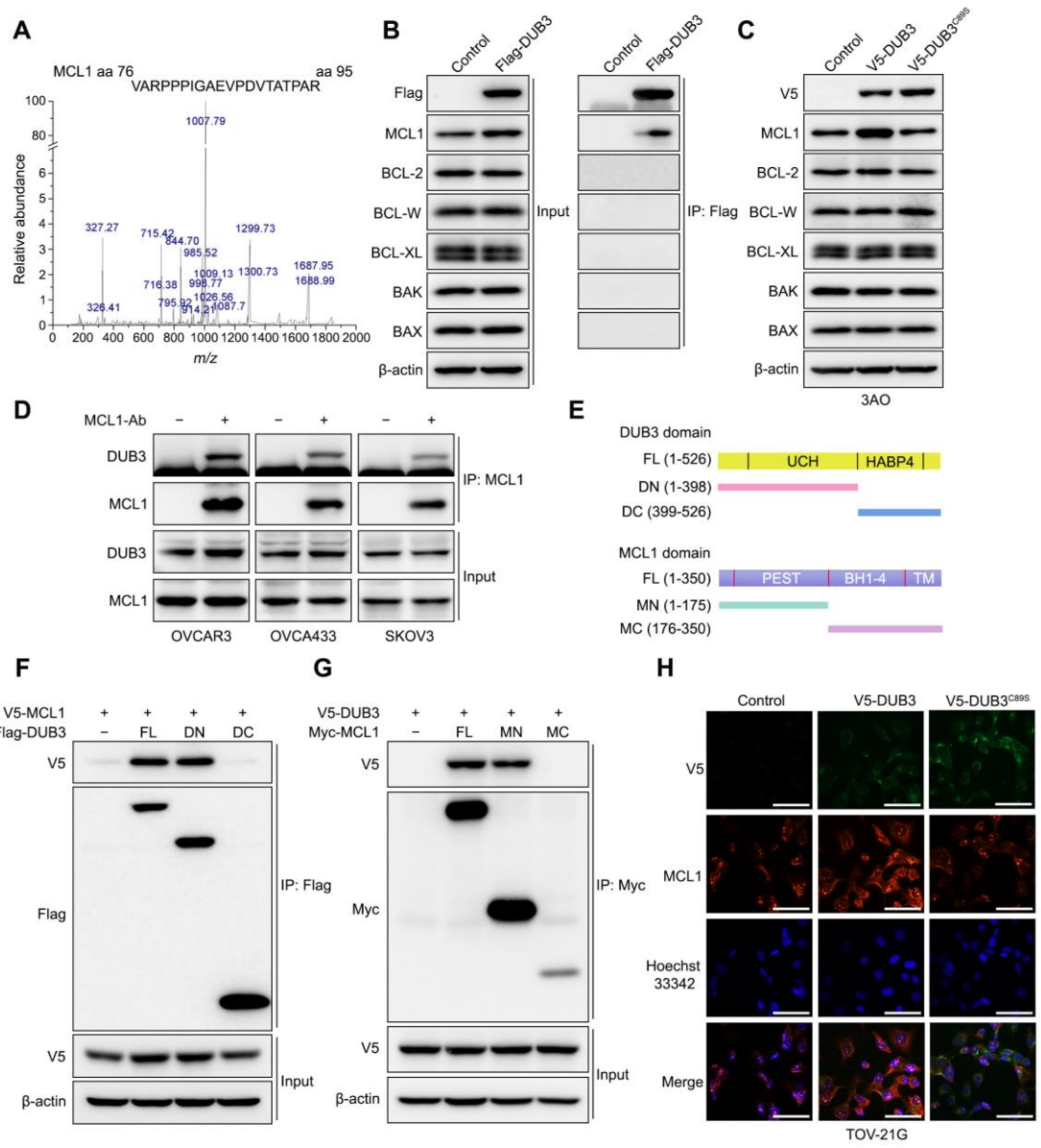

Fig. S2 DUB3 interacts with MCL1 in ovarian cancer cells. (*A*) Representative fragmentation spectrum of the identified MCL1 peptides. aa, amino acid. (*B*) Immunoblotting of the indicated BCL-2 family members in a co-IP assay with anti-Flag agarose beads. (*C*) Immunoblotting analysis of several BCL-2 family members in V5-DUB3 overexpressing 3AO cells. (*D*) Immunoblotting analysis of DUB3 expression in a co-IP assay performed in OVCAR3, OVCA433 or SKOV3 cells with an anti-MCL1 antibody. (*E*) Schematic showing the generation of the DUB3 (full-length (FL), N-terminus (DN) and C-terminus (DC)) and MCL1 (full-length (FL), N-terminus (MN) and C-terminus (MC)) constructs. (*F*) Immunoblotting analysis of V5-MCL1 and Flag-DUB3 expression in a co-IP assay performed in 293T cells with anti-Flag agarose beads. (*G*) Immunoblotting analysis of V5-DUB3 and Myc-MCL1 expression in a co-IP assay performed in 293T cells with an anti-Myc antibody. (*H*) Confocal microscopy detection of the co-localization of V5-DUB3 (green) and MCL1 (red) in TOV-21G cells. Nuclei were stained using Hoechst33342 (blue). Scale bars, 60 μm. Representative results of three biological replicates are shown.

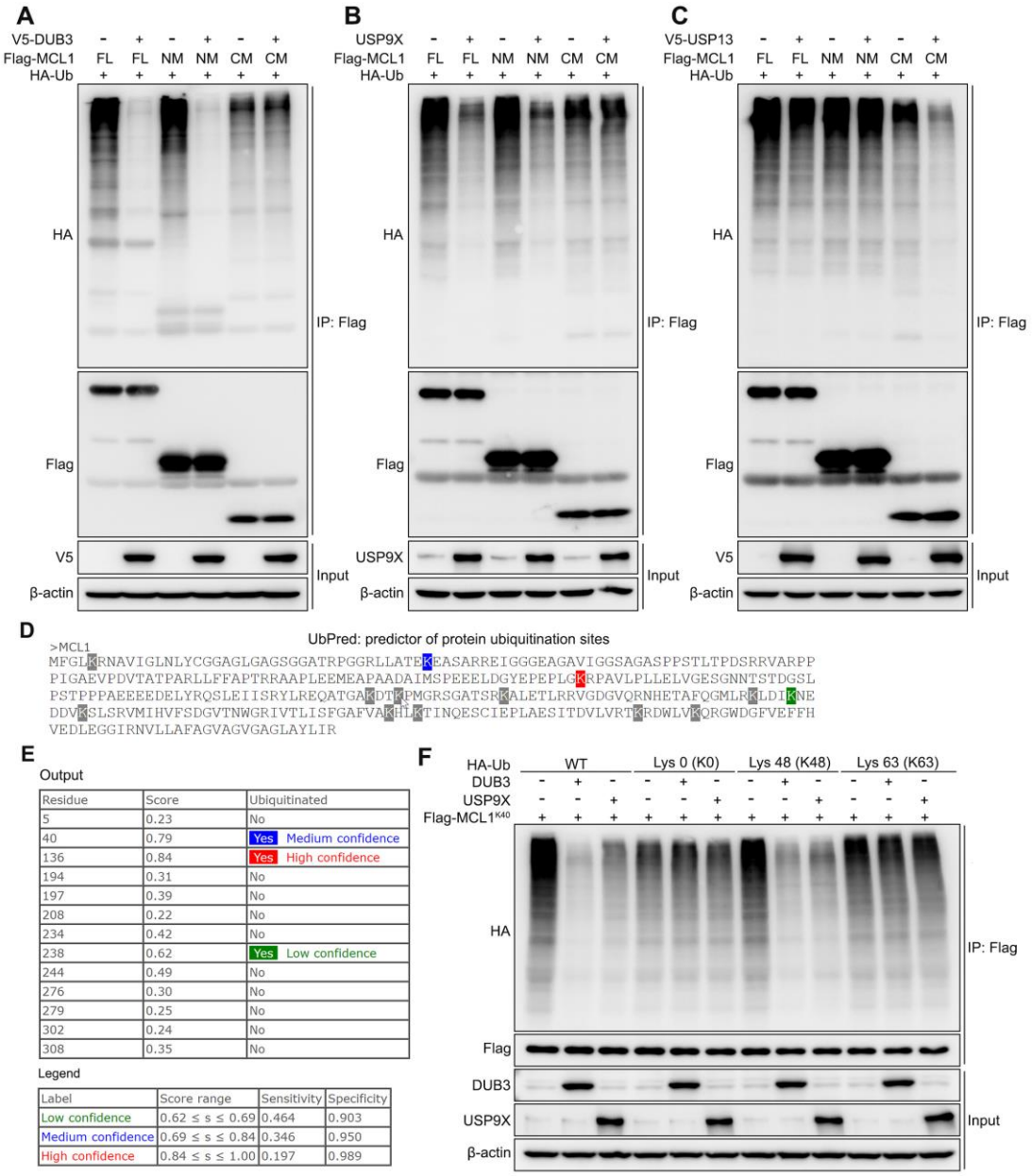

Fig. S3 DUB3 deubiquitinates the N terminus of MCL1. (*A-C*) Immunoblotting to detect the ubiquitination of the MCL1 deletion mutants (FL, NM and CM) in 293T cells co-transfected with Flag-MCL1 (FL, NM and CM), HA-Ubiquitin along with DUB3, USP9X and USP13. (*D*) Ubiquitination ability of all thirteen lysines within MCL1 as evaluated by the UbPred website. (*E*) Individual scores of all thirteen lysines within MCL1. (*F*) Immunoblotting to detect the ubiquitination of MCL1^{K40} in 293T cells co-transfected with Flag-MCL1^{K40}, V5-DUB3, USP9X and HA-Ubiquitin mutant (K0 indicates that all lysines were replaced by arginines, and K48 and K63 indicate that all lysines, except for one lysine at K48 or K63, were mutated to arginines). Representative results of three biological replicates are shown.

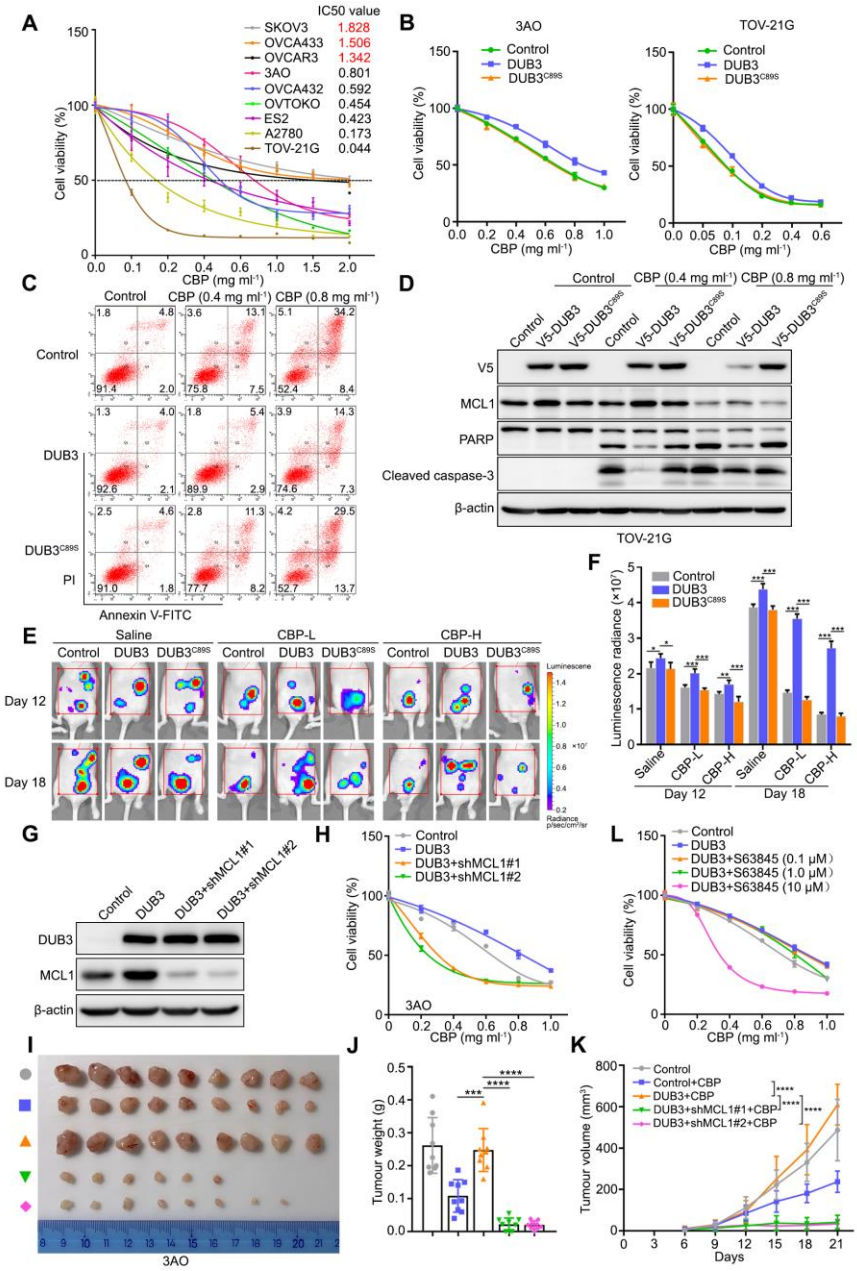

Fig. S4 DUB3 overexpression leads to chemoresistance in ovarian cancer cells. (*A*) Cell viability of nine ovarian cancer cell lines treated with increasing concentrations of carboplatin. (*B*) Cell viability of 3AO and TOV-21G cells expressing an empty vector, DUB3 or DUB3^{C89S} and treated with different doses of CBP. (*C*) Representative results of the flow cytometry experiments shown in Fig. 3*A*. (*D*) Immunoblotting of indicated proteins in TOV-21G cells expressing an empty vector, DUB3 or DUB3^{C89S} and treated with CBP. (*E* and *F*) Representative images and quantification of the luminescence radiance of metastatic nodules in the abdomens of mice injected with 3AO cells expressing an empty vector, DUB3 or DUB^{C89S} and administered CBP (n=5). (*G*) Immunoblotting of DUB3 and MCL1 in 3AO cells overexpressing an empty vector, DUB3, or together with shRNAs targeting MCL1. (*H*) Cell viability of 3AO cells overexpressing an empty vector, DUB3, or together with shRNAs targeting MCL1 following treatment with of CBP. (*I-K*) Images, tumor weight and growth curve of xenografts of 3AO cells expressing an empty vector, DUB3, or together with shRNAs targeting MCL1 (n=9). (*L*) Cell viability of 3AO cells overexpressing an empty vector, DUB3, or together with S63845 treatment. Two-tailed Student's *t*-test; *P<0.05, **P<0.01, ***P<0.001 and ****P<0.0001; error bars indicate the mean±s.d. In *A-D* and *L*, representative results of three biological replicates are shown.

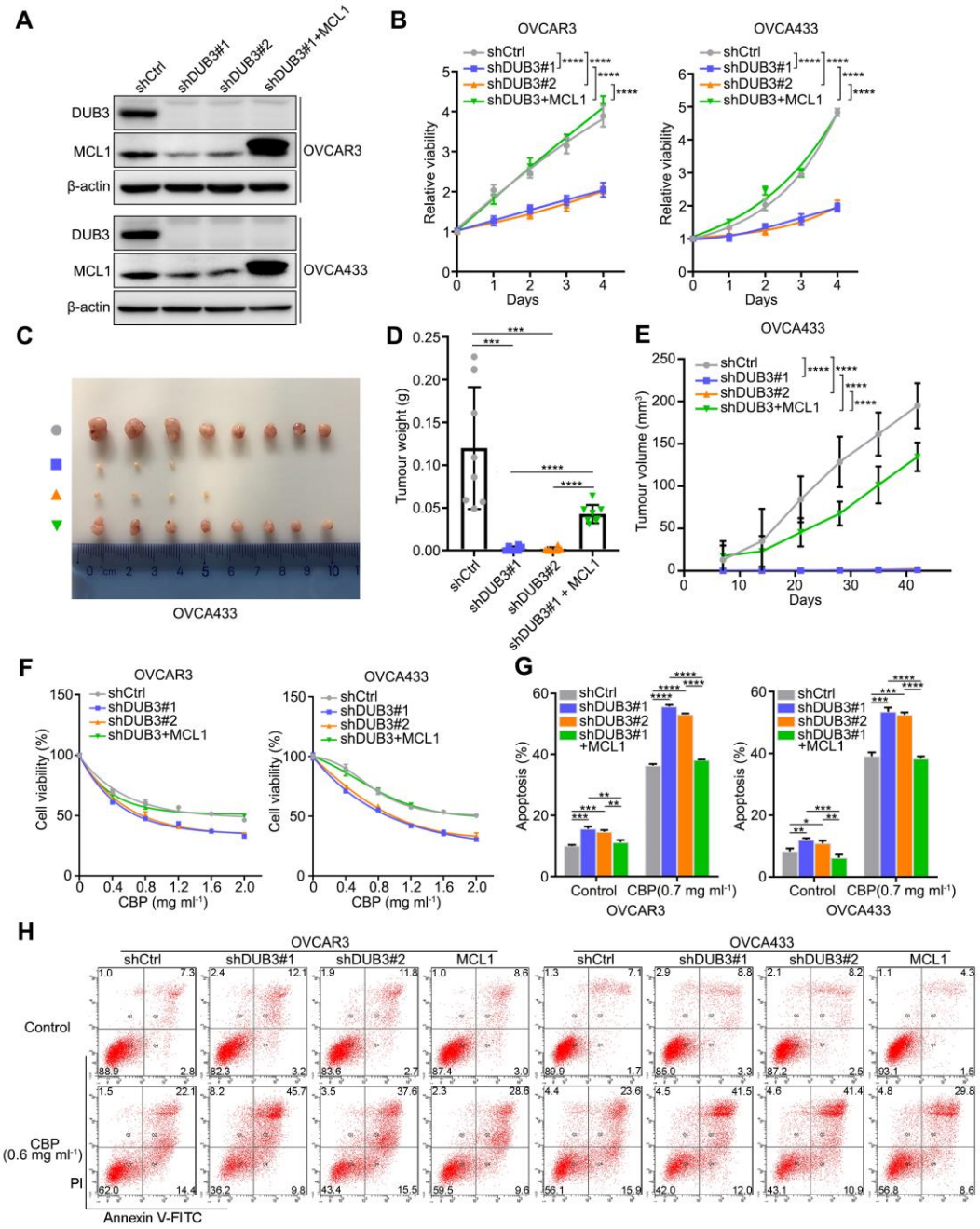

Fig. S5 DUB3 depletion triggers ovarian cancer cell apoptosis via the abolishment of MCL1 protein expression. (*A*) Immunoblotting of DUB3 and MCL1 expression in OVCAR3 and OVCA433 cells expressing non-targeting or DUB3-targeting shRNAs, or together with ectopic MCL1. (*B*) *In vitro* growth of OVCAR3 and OVCA433 cells expressing non-targeting or DUB3-targeting shRNAs, or together with ectopic MCL1. (*C-E*) Tumor image, tumor weights and *in vivo* growth curve of OVCA433 cells expressing non-targeting or DUB3-targeting shRNAs, or together with ectopic MCL1 (n=8). (*F*) Cell viability of OVCAR3 and OVCA433 cells expressing non-targeting or DUB3-targeting shRNAs, or together with ectopic MCL1, following treatment with different doses of CBP. (*G*) Quantitative analysis of the apoptosis rate of OVCAR3 and OVCA433 cells expressing non-targeting or MCL1-targeting shRNAs. (*H*) Representative results of the flow cytometry experiments shown in Fig. S5*G*. Two-tailed Student's *t*-test; *P<0.05, **P<0.01, ***P<0.001 and ****P<0.0001; error bars indicate the mean±s.d. In *A*, *B and F-H*, representative results of three biological replicates are shown.

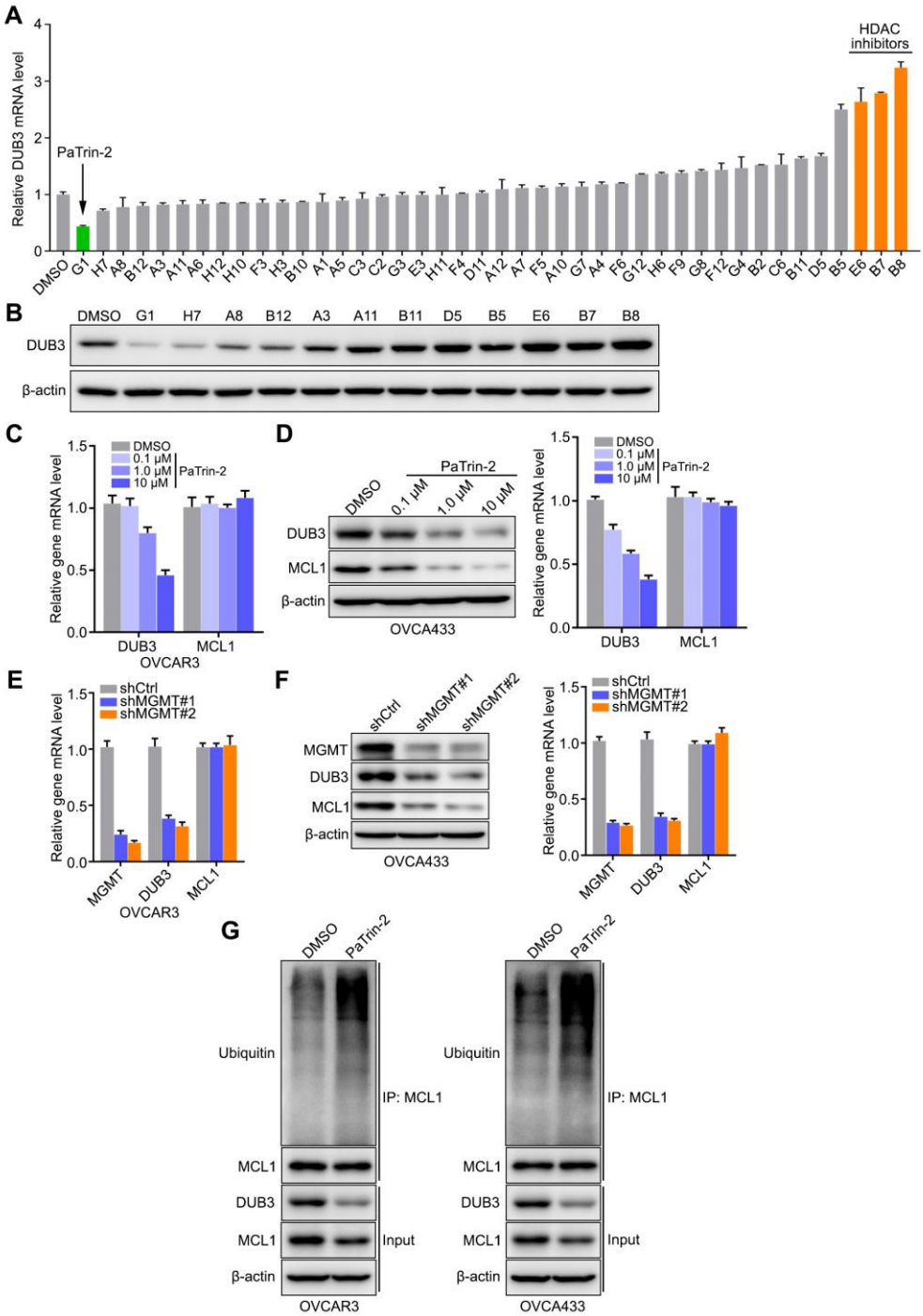

Fig. S6 PaTrin-2 inhibits the MGMT-DUB3-MCL1 axis. (*A* and *B*) qRT-PCR analysis and Immunoblotting of DUB3 expression in OVCA433 cells treated with different inhibitors (10μM). (*C*) qRT-PCR analyses of the mRNA expression levels of DUB3 and MCL1 in OVCAR3 cells treated with different doses of PaTrin-2. (*D*) Immunoblotting and qRT-PCR analyses of the protein and mRNA expression levels of DUB3 and MCL1 in OVCA433 cells treated with different doses of PaTrin-2. (*E*) qRT-PCR analyses of the mRNA expression levels of MGMT, DUB3 and MCL1 in OVCAR3 cells expressing non-targeting shRNA or shRNAs targeting MGMT. (*F*) Immunoblotting and qRT-PCR analyses of the protein and mRNA expression levels of MGMT, DUB3 and MCL1 in OVCA433 cells expressing non-targeting shRNA or shRNAs targeting MGMT. (*G*) Immunoblotting to detect the ubiquitination of MCL1 in OVCAR3 and OVCA433 cells treated with PaTrin-2 (10μM). Error bars indicate the mean±s.d., representative results of three biological replicates are shown.

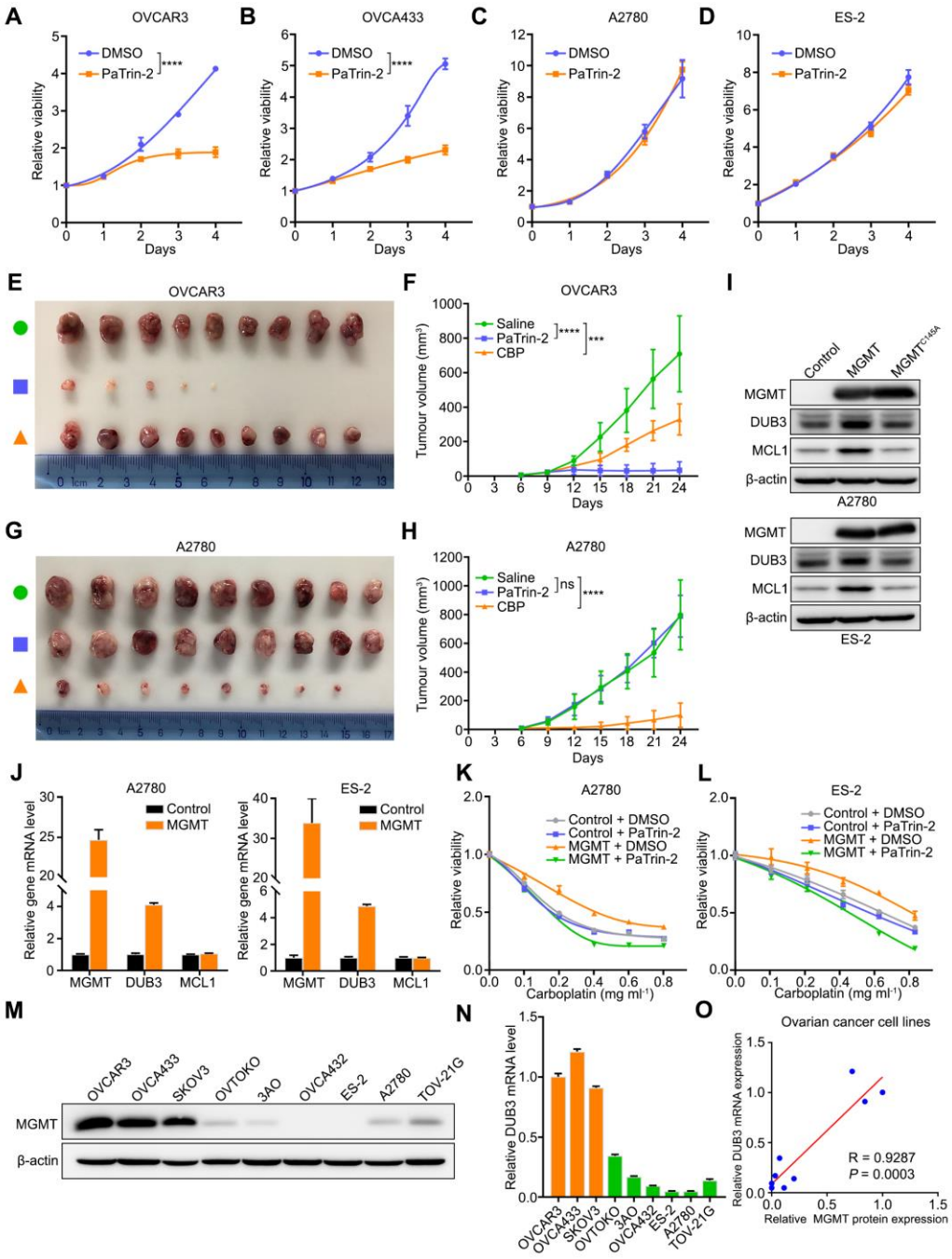

Fig. S7 (*A-D***)** *In vitro* proliferation of OVCAR3, OVCA433, A2780 and ES-2 cells treated with DMSO or PaTrin-2 (10μM) for 5 consecutive days. Error bars indicate the mean±s.d. Representative results of three biological replicates are shown. (*E-H*) Images and *in vivo* growth of xenografts of OVCAR3 and A2780 cells treated with saline, PaTrin-2 or CBP. Error bars indicate the mean±s.d. (n=9). (*I*) Immunoblotting of MGMT, DUB3 and BCL-2 family member expression in A2780 and ES-2 cells expressing an empty vector, MGMT or MGMT^{C145A}. (*J*) qRT-PCR analysis of MGMT, DUB3 and MCL1 expression in A2780 and ES-2 cells expressing an empty vector or ectopic MGMT. (*K* and *L*) Cell viability of A2780 and ES-2 cells expressing an empty vector or ectopic MGMT and treated with DMSO or PaTrin-2 (10μM) along with different doses of CBP. (*M* and *N*) Immunoblotting and qRT-PCR analysis of MGMT expression in ovarian cancer cell lines. (*O*) Correlation analysis of MGMT protein and DUB3 mRNA expression in ovarian cancer cell lines. Pearson correlation coefficients are shown. Error bars indicate the mean±s.e.m. of three biological replicates. Two-tailed Student's *t*-test; ***P<0.001 and ****P<0.0001.

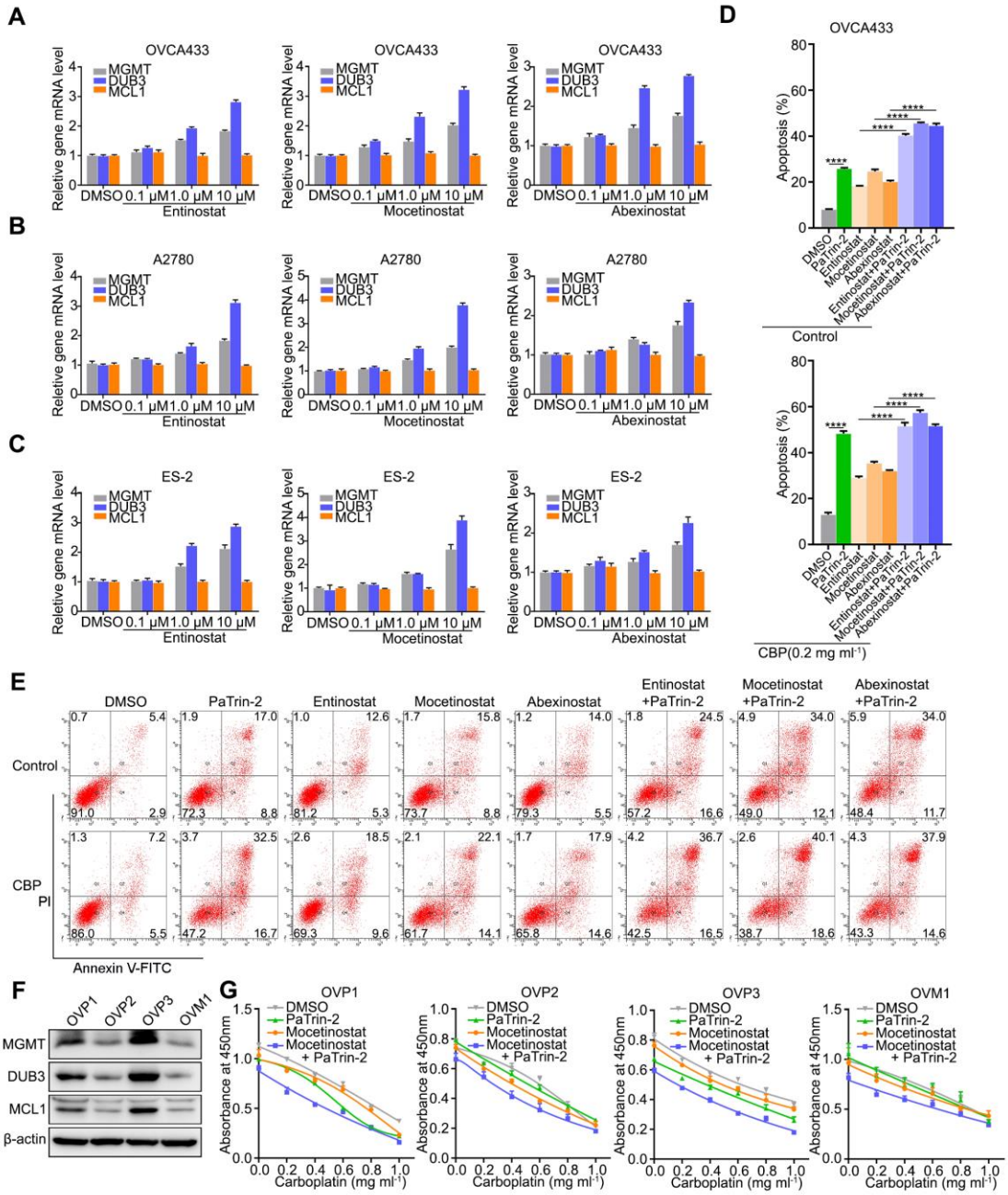

Fig. S8 HDACis activate MGMT at the transcriptional level. (*A-C*) qRT-PCR analysis of the mRNA expression levels of MGMT, DUB3 and MCL1 in OVCA433, A2780 and ES-2 cells treated with different doses of Entinostat, Mocetinostat or Abexinostat. (*D*) Quantitative analysis of apoptosis rates of OVCA433 cells treated with DMSO, Entinostat (10μM), Mocetinostat (10μM) or Abexinostat (10μM) either alone or together with PaTrin-2 (10μM) following the administration of CBP. (*E*) Representative images of Annexin V/ FITC double staining of OVCA433 cells treated with DMSO, Entinostat (10μM), Mocetinostat (10μM) or Abexinostat (10μM) either alone or together with PaTrin-2 (10μM) following the administration of CBP. (*F*) Immunoblotting of MGMT, DUB3 and MCL1 expression in OVP1, OVP2, OVP3 and OVM1 cells. (*G*) Cell viability detection at an absorbance of 450 nm in the indicated primary cell lines treated with DMSO, Entinostat, Mocetinostat or Abexinostat either alone or together with PaTrin-2 following the administration of CBP. In *A-C*, the error bars indicate the mean±s.e.m. of three biological replicates. In *D-G*, the error bars indicate the mean±s.d., representative results of three biological replicates were shown. Two-tailed Student's *t*-test; ****P<0.0001.

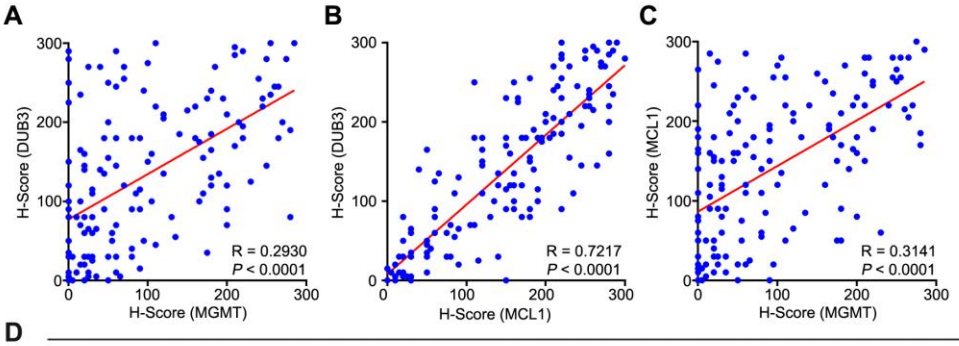

D

Clinical variable		DUB3 (±SE)	*P* value	MCL1 (±SE)	*P* value	MGMT (±SE)	*P* value
Age at diagnosis	<56	130.7 ± 10.07, n=74	0.8777	141.0 ± 10.04, n=74	0.9801	82.70 ± 9.356, n=74	0.0785
	⩾56	133.0 ± 11.42, n=76		141.4 ± 10.79, n=76		108.0 ± 10.72, n=76	
2014 FIGO stage	III	128.6 ± 8.431, n=118	0.4173	138.4 ± 8.177, n=118	0.4648	95.93 ± 7.883, n=118	0.8938
	IV	143.8 ± 17.50, n=32		151.6 ± 16.81, n=32		93.59 ± 16.84, n=32	
Residual tumor size (cm)	<2	120.2 ± 8.508, n=109	0.0117	134.7 ± 8.662, n=109	0.1487	87.71 ± 8.269, n=109	0.0767
	⩾2	162.9 ± 15.31, n=41		158.5 ± 13.7, n=41		116.2 ± 14.03, n=41	
Level of CA125 in	<500	106.6 ± 14.59, n=37	0.0093	115.8 ± 14.31, n=37	0.0478	80.54 ± 14.65, n=37	0.2344
primary tumors (U/ml)	⩾500	140.1 ± 8.782, n=113		149.5 ± 8.449, n=113		100.4 ± 8.22, n=113	
Recurrent type	Sensitive	86.22 ± 7.705, n=86	<0.0001	92.44 ± 7.615, n=86	<0.0001	67.91 ± 7.308, n=86	<0.0001
(Platinum)	Resistant	193.2 ± 10.41, n=64		206.7 ± 8.696, n=64		132.6 ± 12.28, n=64	

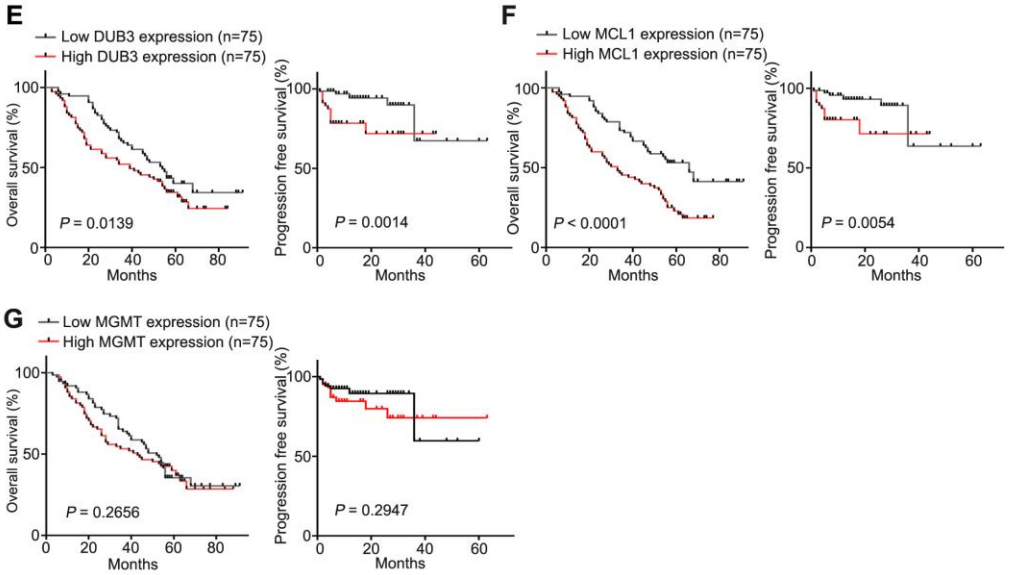

Fig. S9 MGMT-DUB3-MCL1 expression is correlated with chemoresistance in ovarian cancer. (A-C) Correlation analysis of MGMT and DUB3 expression levels, DUB3 and MCL1 expression levels, and MGMT and MCL1 expression levels. Pearson correlation coefficients are shown. (*D*) Correlation analysis of the MGMT, DUB3 and MCL1 expression levels and pathological variables. Two-tailed Student's *t*-test. (*E-G*) Correlations between DUB3, MCL1 or MGMT expression and overall survival or progression-free survival in ovarian cancer patients. Kaplan-Meier survival plots are shown.

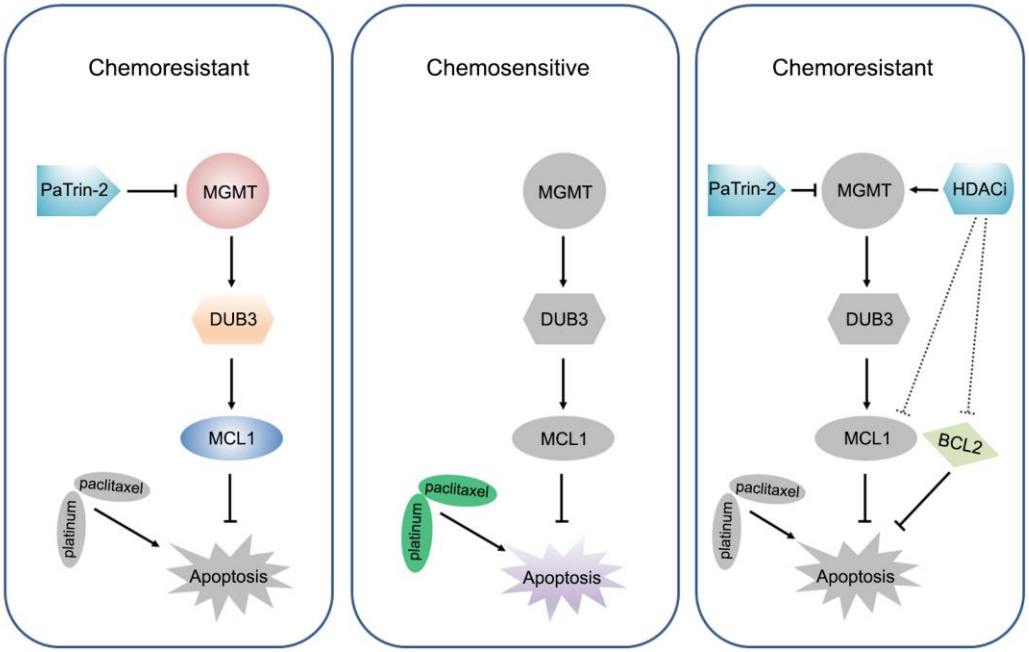

Fig. S10 Schematic showing the three chemoresistance statuses of ovarian cancer. Left: ovarian cancer cases with high expression of the MGMT-DUB3-MCL1 axis that are resistant to standard chemotherapy; administration of PaTrin-2 alone significantly inhibits tumor growth. Middle: ovarian cancer cases with low expression of the MGMT-DUB3-MCL1 axis that are sensitive to the standard chemotherapy regimen. Right: ovarian cancer cases with low MGMT-DUB3-MCL1 expression that are resistant to standard chemotherapy due to the high expression of other anti-apoptotic proteins, such as BCL-2; the combined administration of HDACis and PaTrin-2 has a synthetic therapeutic effect.

Table S1 The peptide numbers of the BCL-2 family proteins associated with Flag-DUB3.

Protein	Number of the peptides
DUB3	41
MCL1	24
BAD	0
BAK	0
BAP31	0
BAX	0
BCL-2	0
BCL-2A1	0
BCLB	0
BCL-B	0
BCL-G	0
BCL-RAMBO	0
BCL-W	0
BCLX	0
BCL-XL	0
BECLIN-1	0
BFK	0
BFL-1	0
BID	0
BIK	0
BIM	0
BMF	0
BNIP1	0
BNIP-3	0
BOK	0

HRK	0
NIX	0
NOXA	0
PUMA	0

Table S2 Characters of primary cell lines.

	OVP1	OVP2	OVP3	OVM1
Patient Age	37	49	46	56
Location	Primary ovarian cancer	Primary ovarian cancer	Primary ovarian cancer	Peritoneal carcinomatosis
Grade	High	High	High	High
Differentiation	Poor	Poor	Poor	Poor
Histologic Type	Serous adenocarcinoma	Serous adenocarcinoma	Serous adenocarcinoma	Serous adenocarcinoma

Table S3 Information of SMIs used in this study.

Number	Inhibitor Name	Cat. No.
A1	HLCL-61 (hydrochloride)	HY-100025A
A3	UNC0321	HY-10930
A4	UNC0638	HY-15273
A5	I-BRD9	HY-18975
A6	EPZ015866	HY-100235
A7	OF-1	HY-12518
A8	A-366	HY-12583
A10	SGC707	HY-19715
A11	UNC0642	HY-13980
A12	UNC0379	HY-12335
B2	Inauhzin	HY-15869
B5	UNC1999	HY-15646
B7	Entinostat	HY-12163
B8	Mocetinostat	HY-12164
B10	PFI-1	HY-16586
B11	Pimelic Diphenylamide 106 (analog)	HY-19430
B12	OTX-015	HY-15743
C2	GSK1324726A	HY-13960
C3	PFI-2 (hydrochloride)	HY-18627A
C6	GSK503	HY-12856
D5	EX-527	HY-15452
D11	BI 2536	HY-50698
E3	BRD4770	HY-16705
E6	PCI-24781	HY-10990
F3	JIB-04	HY-13953
F4	MS436	HY-13959

F5	SRT 1720 (Hydrochloride)	HY-15145
F6	EPZ011989	HY-16986
F9	4SC-202 (free base)	HY-16012A
F12	Dacinostat	HY-13606
G1	Lomeguatrib	HY-13668
G3	Parthenolide	HY-N0141
G4	Bromosporine	HY-15815
G7	SGI-1027	HY-13962
G8	Scriptaid	HY-15489
G12	(R)-(-)-JQ1 Enantiomer	HY-13030A
H3	GSK 525762A	HY-13032
H6	Pracinostat	HY-13322
H7	Tenovin-1	HY-13423
H10	(+)-JQ-1	HY-13030
H11	MM-102 (trifluoroacetate)	HY-12220A
H12	Zebularine	HY-13420